PROCEEDINGS OF SCIENCE

# Form factor curves consistent with unitarity for semileptonic decays

**Callum Radley-Scott,**[a,*] **Jonathan M Flynn**[a] **and Nikolai Husung**[b,c]

[a] *Physics and Astronomy, University of Southampton, Southampton SO17 1BJ, United Kingdom*

[b] *Instituto de Física Teórica UAM-CSIC, C/ Nicolás Cabrera 13-15, Universidad Autónoma de Madrid, Cantoblanco 28049 Madrid, Spain*

[c] *Departamento de Física Teórica, Universidad Autónoma de Madrid, Cantoblanco 28049 Madrid, Spain*

*E-mail:* c.j.radley-scott@soton.ac.uk, j.m.flynn@soton.ac.uk, nikolai.husung@uam.es

We discuss a method to generate form factor curves consistent with dispersive constraints across the entire kinematic range for exclusive semileptonic (SL) pseudoscalar to pseudoscalar decays, for example $B \to \pi \ell \nu$ and $B_s \to K \ell \nu$. The work builds on the Dispersive Matrix (DM) method which allows model-independent extrapolation to any desired $q^2$ value in the SL physical region using known form factor information at specific discrete $q^2$ points as input. Here $q$ is the outgoing lepton-pair 4-momentum. An obstacle in using DM results for phenomenological predictions, such as forward-backward asymmetries, is that it is not obvious how to use the bounds over continuous ranges of $q^2$ when integrating, for example, the differential decay rate over the physical $q^2$ range or over bins in $q^2$. We describe a method to generate a family of curves, each consistent with unitarity constraints, that can be used in the same way as a set generated from a parametrized fit (e.g. a $z$-fit). This allows integration over any desired bins. We further show some techniques to increase the computational efficiency of the method. We demonstrate the application to determining $|V_{ub}|$.

*The 41st International Symposium on Lattice Field Theory,*
*July 28 - August 3, 2024*
*University of Liverpool, Liverpool, United Kingdom*

*Speaker





PoS(LATTICE2024)253

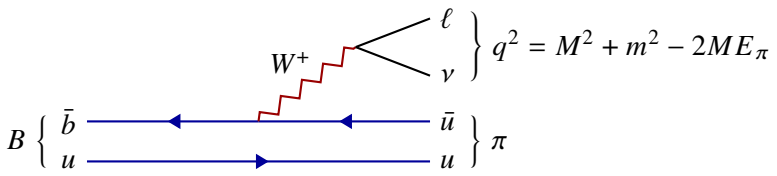


**Figure 1:** Quark flow diagram for $B \to \pi\ell\nu$ decay

## 1. Background

We consider exclusive semileptonic pseudoscalar to pseudoscalar decays, specifically $B \to \pi\ell\nu$ and $B_s \to K\ell\nu$, for which the QCD matrix element, written for $B$ to $\pi$ decay, is

$$\langle \pi(k) \,|\mathcal{V}^\mu(0)|\, B(p)\rangle = f_+(q^2)\left(p^\mu + k^\mu - \frac{M^2-m^2}{q^2}q^\mu\right) + f_0(q^2)\frac{M^2-m^2}{q^2}q^\mu. \tag{1}$$

Here, $\mathcal{V}^\mu = \bar{u}\gamma^\mu b$ is the weak flavour-changing current. $B$ and $\pi$ have masses $M$ and $m$, with 4-momenta $p$ and $k$, respectively, and $q = p - k$. The form factors $f_+$ and $f_0$ satisfy the kinematic constraint $f_+(0) = f_0(0)$. We wish to find the full $q^2$ dependence of the form factors. For these heavy-to-light decays, lattice simulations give form factor data in the high-$q^2$ (low-recoil) regime which must be extrapolated (in contrast, sum rules provide values at low $q^2$).

Bounds on the form factors are obtained from dispersion relations. They relate a two-point current-current correlator, projected onto its $J^P = 1^-$ or $0^+$ channels, to an integral of its absorptive part, in which a complete sum of exclusive states is inserted.

$$\begin{gathered}\chi_{0^+} = \frac{1}{\pi}\int_{t_{cut}}^{\infty} dt\, \frac{\mathrm{Im}\,\Pi_{0^+}(t)}{t}, \qquad \chi_{1^-} = \frac{1}{\pi}\int_{t_{cut}}^{\infty} dt\, \frac{\mathrm{Im}\,\Pi_{1^-}(t)}{t^2}, \\ \mathrm{Im}\,\Pi_{0^+,1^-} = \frac{1}{2}\sum_n \int d\mu(n)(2\pi)^4\delta^{(4)}(q-p_n)|\langle 0|J|n\rangle|^2.\end{gathered} \tag{2}$$

Restricting the sum of states (and using crossing symmetry) leads to the bounds [1–8].

We introduce the conformal map, $z$, which maps the $q^2 = t$ complex plane onto the unit disc:

$$z(t) = \frac{\sqrt{t_{\rm cut} - t} - \sqrt{t_{\rm cut} - t_0}}{\sqrt{t_{\rm cut} - t} + \sqrt{t_{\rm cut} - t_0}}, \qquad t_0 = t_{\rm cut} - \sqrt{t_{\rm cut}(t_{\rm cut} - (M-m)^2)}, \tag{3}$$

where $t_{\rm cut}$ is the relevant two-particle production threshold and we have chosen $t_0$ to make the range of $z$ symmetric around 0 for the kinematically allowed range of $q^2$. The dispersive bounds then take the form

$$\frac{1}{2\pi i}\oint_{|z|=1}\frac{dz}{z}|\phi(z)B(z)f(z)|^2 \le \chi, \tag{4}$$

where $\phi(z)$ is the outer function containing kinematic factors, and $B(z)$ is a Blaschke factor that ensures analyticity in the presence of sub-threshold poles.

There are two common ways to proceed:

- Analyticity allows a power series expansion of $\phi B f$ (BGL/BCL expansion) and unitarity gives constraints on the coefficients [5–7].
- The Dispersive Matrix method finds form factor values allowed by unitarity, independent of any functional form [1–4, 8–11].

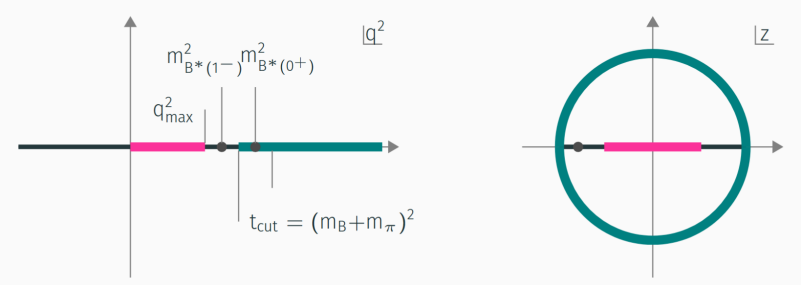


**Figure 2:** Mapping the $q^2$ complex plane onto the unit disc in $z$.

## 2. Dispersive Matrix (DM) Method

We define an inner product,

$$\langle j \,|\, k \rangle = \frac{1}{2\pi i} \oint_{|z|=1} \frac{dz}{z} \bar{j}(z) k(z), \tag{5}$$

together with function $g_t(z)$,

$$g_t(z) \equiv \frac{1}{1 - \bar{z}(t) z}, \tag{6}$$

so that $\langle g_t \,|\, \phi B f \rangle = \phi\big(z(t)\big) B\big(z(t)\big) f\big(z(t)\big)$. We introduce the Gram matrix,

$$M = \begin{pmatrix} \langle \phi B f \,|\, \phi B f \rangle & \langle \phi B f \,|\, g_t \rangle & \langle \phi B f \,|\, g_{t_1} \rangle & \cdots & \langle \phi B f \,|\, g_{t_n} \rangle \\ \langle g_t \,|\, \phi B f \rangle & \langle g_t \,|\, g_t \rangle & \langle g_t \,|\, g_{t_1} \rangle & \cdots & \langle g_t \,|\, g_{t_n} \rangle \\ \langle g_{t_1} \,|\, \phi B f \rangle & \langle g_{t_1} \,|\, g_t \rangle & \langle g_{t_1} \,|\, g_{t_1} \rangle & \cdots & \langle g_{t_1} \,|\, g_{t_n} \rangle \\ \vdots & \vdots & \vdots & \ddots & \vdots \\ \langle g_{t_n} \,|\, \phi B f \rangle & \langle g_{t_n} \,|\, g_t \rangle & \langle g_{t_n} \,|\, g_{t_1} \rangle & \cdots & \langle g_{t_n} \,|\, g_{t_n} \rangle \end{pmatrix} = \begin{pmatrix} \langle \phi B f \,|\, \phi B f \rangle & \vec{F}^{\mathrm{T}} \\ \vec{F} & G \end{pmatrix} \tag{7}$$

with $\vec{F} = \big(\langle \phi B f \,|\, g_t \rangle, \langle \phi B f \,|\, g_{t_1} \rangle, \ldots, \langle \phi B f \,|\, g_{t_n} \rangle\big)$. Here, $\langle \phi B f \,|\, \phi B f \rangle$ is the inner product constrained by the dispersion relation $\chi \geq \langle \phi B f \,|\, \phi B f \rangle$, $\langle \phi B f \,|\, g_t \rangle$ contains the form factor $f(t)$ which we wish to find, and $\langle \phi B f \,|\, g_{t_i} \rangle$ contain the known form factor values at points $q_i^2 = t_i$. Since $M$ and $G$ are both positive semidefinite (and $\det G > 0$ provided $t$ and all the $t_i$ are distinct), the identity $\det M = \det G \times \big(\langle \phi B f \,|\, \phi B f \rangle - \vec{F}^{\mathrm{T}} G^{-1} \vec{F}\big)$ leads to

$$\langle \phi B f \,|\, \phi B f \rangle - \vec{F}^{\mathrm{T}} G^{-1} \vec{F} \geq 0. \tag{8}$$

Substituting the dispersive bound gives

$$\chi - \vec{F}^{\mathrm{T}} G^{-1} \vec{F} \geq 0. \tag{9}$$

The left hand side is a quadratic polynomial in $\phi(t) B(t) f(t)$ and the inequality provides a lower and an upper bound on $f(t)$.

## 3. Generating curves

The DM method makes it easy to find form-factor bounds at any $q^2$, but it is not so obvious how to exploit the bounds over continuous ranges of $q^2$ when, for example (partially) integrating the differential decay rate.

We describe how to apply the DM method to generate a family of curves, each consistent with the unitarity constraints, that can be used in the same way as a set generated from a parameterised fit (e.g. a $z$-fit). We do this assuming perfect knowledge of the form factors at a set of input $q^2$ values. By resampling the inputs we can generate further sets of curves to take into account errors in the inputs. For each resampling we generate $n_{\text{inner}}$ curves.

The first step is to find the bounds at $q^2 = 0$ and implement the kinematic constraint, following the method described in [9]. We separately determine the bounds for $f_+$ and $f_0$ at $q^2 = 0$ and then randomly and uniformly select a value in the intersection of these bounds as the common $f_+(0) = f_0(0)$ (whenever a unitarity bound for a form factor is computed, our assumption is that the form factor value is uniformly distributed across the bound). From here on both form factors are treated in the same way and our discussion will apply for either one.

With the point at $q^2 = 0$ chosen, we have constrained our attention to all form factor curves passing through this point. The extra point is added as new input in the dispersive matrix, allowing us to determine a new bound at $q^2 = \delta$, where $\delta$ is small. We randomly choose a value satisfying the bound, add the $q^2 = \delta$ point to the dispersive matrix and compute bounds at $q^2 = 2\delta$. We repeat this process to step across the entire physical $q^2$ region.

In the limits $n_{\text{inner}} \to \infty$ and $\delta \to 0$ we will construct all form factor curves allowed by unitarity which pass through the resampled input points (and satisfy the kinematic constraint). In practice we keep $\delta$ finite and compute an interpolating function through the generated points. We must therefore check that $\delta$ can be made small enough for it not to affect phenomenological quantities computed using the generated curves (and check for independence of the interpolation method).

Figure 3 shows $n_{\text{inner}} = 100$ form factor curves for $f_+$ and $f_0$ generated from a single resample of JLQCD [12] synthetic lattice QCD data points for $B \to \pi l \nu$ decay. The DM method bounds are overlaid and the envelope of all curves is within, but is filling out, the bounds.

### 3.1 'Marching' across the full $q^2$ range

When generating form factor curves over the full $q^2$ range, the size and number of dispersive matrices increases, more so as $\delta$ decreases.

However, the upper and lower bounds for adding new points to a curve become closer and closer and effectively coalesce as more points are added. This is because almost all freedom in the curve is exhausted after sufficiently many points have been chosen. We find that we can remove earlier points from the dispersive matrix provided we check that the width of the bound for a new point remains close enough to zero. This speeds up the generation of curves; the dispersive matrix does not keep growing in size and we 'march' across the range of $q^2$.

In practice, a threshold is set below which the width of the bound is considered to be zero. If the width is above the threshold, then we do not drop an earlier point before computing the next set of bounds. We check that we can make the threshold small enough for it not to affect phenomenological results.

### 3.2 Dependence on $\delta$

Figure 4 shows how $\Gamma/|V_{ub}|^2$, the calculated decay rate with the CKM factor removed, changes as $\delta$ is varied. We see stability as $\delta$ is decreased and that the effects of nonzero $\delta$ are much smaller than the variations allowed by unitarity.

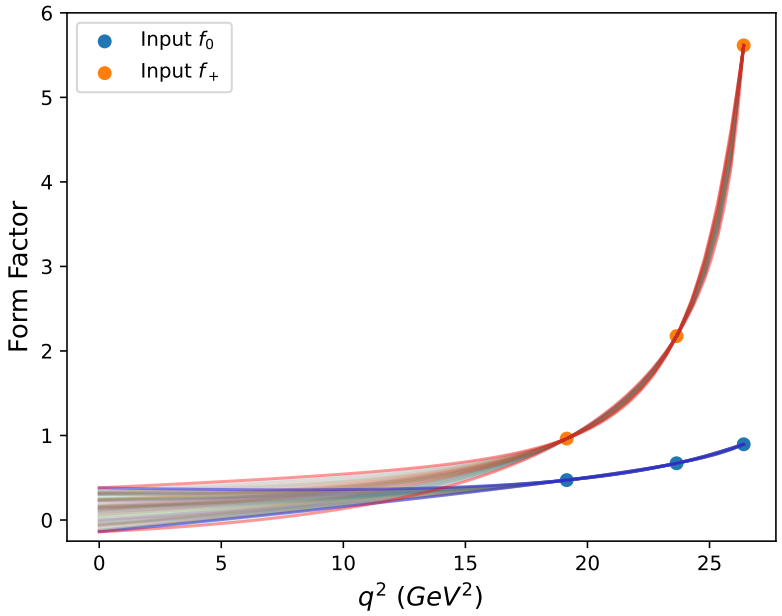


**Figure 3:** 100 curves (plotted in various colours so they can be distinguished from one another) generated for a single resample of JLQCD $B \to \pi \ell \nu$ synthetic data points (orange for $f_+$, blue for $f_0$) [12]. The DM method bounds for these points are also plotted.

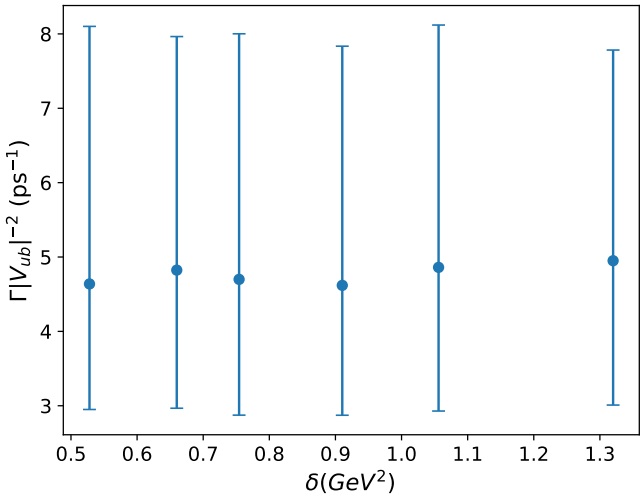


**Figure 4:** Calculation of $\Gamma|V_{ub}|^{-2}$ using 500 form factor curves for various values of $\delta$. The error bars represent the 16th and 84th percentile values, and the point shown is the median.

| Experiment | $10^3\|V_{ub}\|$ DM curves | $10^3\|V_{ub}\|$ BCL $z$-fit |
|---|---|---|
| Belle 2010 | 4.05(43) | 4.10(45) |
| Belle 2013 | 4.14(52) | 3.91(45) |
| BaBar 2010 | 3.55(39) | 3.58(41) |
| BaBar 2012 | 3.97(48) | 4.04(43) |
| All experiments | 3.88(38) | 3.93(41) |
| All experiments excl. BaBar 2010 | 4.08(45) | 4.01(42) |

**Table 1:** $|V_{ub}|$ from $B \to \pi\ell\nu$ using lattice form-factor inputs from JLQCD [12] and experimental datasets from BaBar and Belle [13–16]. We show our results and those from BCL $z$-fits [12] with the same inputs.

### 3.3 Extraction of $V_{ub}$

We consider the extraction of $|V_{ub}|$ using JLQCD [12] $B \to \pi l\nu$ form factors and four sets of experimental results [13–16] from BaBar and BELLE, each of which provides partial branching fractions for a set of $q^2$ bins, with associated covariance matrices.

We will adopt a Bayesian approach. For each $f_+$, $f_0$ curve pair, $c$, and set of experimental results, we compute a likelihood for $|V_{ub}|$ to take the value $\theta$, proportional to $\exp[-\chi^2_c(\theta)/2]$, where

$$\chi^2_c(\theta) = \sum_{\text{expts, } e} \left(\vec{\Delta}_e - \theta^2\vec{\Delta}^0_c\right)^{\mathrm{T}} C_e^{-1} \left(\vec{\Delta}_e - \theta^2\vec{\Delta}^0_c\right). \tag{10}$$

Here $\vec{\Delta}_e$ is a vector of experimental partial branching fractions for a set of $q^2$ bins for experiment $e$, while $\vec{\Delta}^0_c$ are the corresponding quantities, without the CKM factor, computed using the curve pair $c$. $C_e$ is the experimental covariance matrix. The posterior distribution for $\theta$ is then

$$\rho(\theta) = \frac{\sum_c \exp[-\chi^2_c(\theta)/2]}{\sum_c \int_{\theta_0}^{\theta_1} \exp[-\chi^2_c(\theta)/2]\, d\theta}, \tag{11}$$

from which we can evaluate the expectation value for some function $g$ of $\theta$ according to

$$\hat{g} = \int_{\theta_0}^{\theta_1} g(\theta)\rho(\theta)\, d\theta. \tag{12}$$

In particular we can evaluate the mean and variance of $\theta$ to provide an estimated $|V_{ub}|$. We are assuming a uniform prior for $\theta$ in the range $[\theta_0, \theta_1]$. We checked that several choices of the range did not change our results within the accuracy quoted. Table 1 and figure 5 show results for $|V_{ub}|$ for different combinations of experimental inputs. The table also shows the compatibility of our results with those obtained by JLQCD [12] from a BCL $z$-fit to the same inputs.

The variation from resampling the input form factor values when computing phenomenological results is bigger than the variation seen by changing $n_{\text{inner}}$. Hence we performed the above analysis by generating one curve for each resample and increasing the number of resamplings. We used 1760 form-factor curve pairs.

In conclusion we have demonstrated a method to generate form factor curves as functions of $q^2$ which satisfy dispersive unitarity constraints and can easily be used in phenomenology, maintaining the DM matrix method's feature that no functional form needs to be imposed in advance.

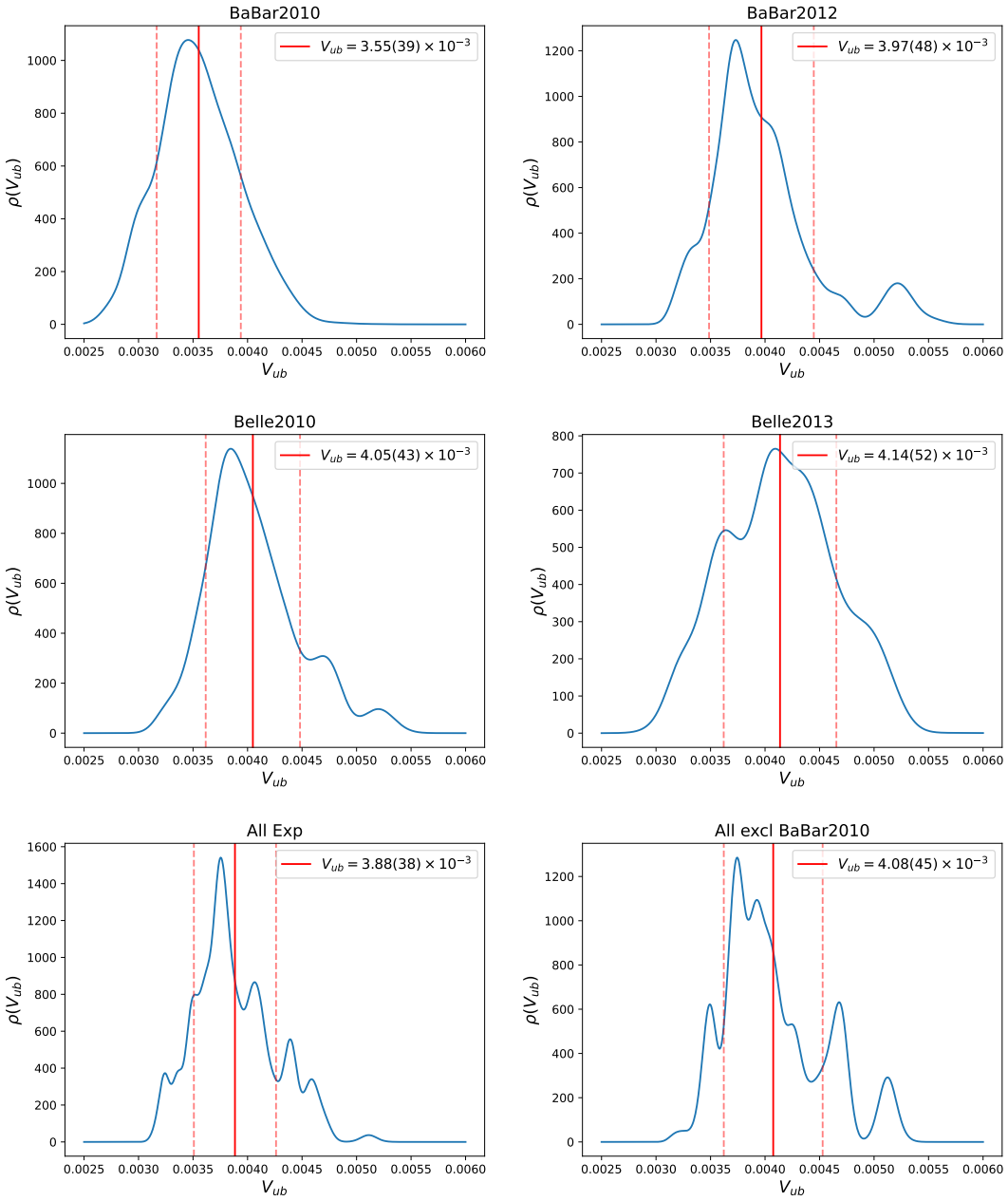


**Figure 5:** Bayesian posterior distributions in blue of $|V_{ub}|$ for various experimental datasets [13–16]. Mean and standard deviation are indicated by vertical red lines and dashed lines.

## References


[1] S. Okubo, *Exact bounds for $K_{l3}$ decay parameters*, *Phys. Rev. D* **3** (1971) 2807.

[2] S. Okubo, *New improved bounds for $K_{l3}$ parameters*, *Phys. Rev. D* **4** (1971) 725.

[3] S. Okubo and I.-F. Shih, *Exact inequality and test of chiral SW(3) theory in $K_{l3}$ decay problem*, *Phys. Rev. D* **4** (1971) 2020.

[4] C. Bourrely, B. Machet and E. de Rafael, *Semileptonic decays of pseudoscalar particles ($M \to M' \ell \nu_\ell$) and short distance behaviour of quantum chromodynamics*, *Nucl. Phys.* **B189** (1981) 157.

[5] C. Bourrely, I. Caprini and L. Lellouch, *Model-independent description of $B \to \pi l \nu$ decays and a determination of $|V_{ub}|$*, *Phys. Rev.* **D79** (2009) 013008 [0807.2722].

[6] C.G. Boyd, B. Grinstein and R.F. Lebed, *Model independent determinations of $B \to D l \nu$, $D^* l \nu$ form-factors*, *Nucl. Phys.* **B461** (1996) 493 [hep-ph/9508211].

[7] C.G. Boyd, B. Grinstein and R.F. Lebed, *Precision corrections to dispersive bounds on form-factors*, *Phys. Rev.* **D56** (1997) 6895 [hep-ph/9705252].

[8] L. Lellouch, *Lattice constrained unitarity bounds for $\bar{B}^0 \to \pi^+ l^- \bar{\nu}$ decays*, *Nucl. Phys.* **B479** (1996) 353 [hep-ph/9509358].

[9] M. Di Carlo, G. Martinelli, M. Naviglio, F. Sanfilippo, S. Simula and L. Vittorio, *Unitarity bounds for semileptonic decays in lattice QCD*, *Phys. Rev. D* **104** (2021) 054502 [2105.02497].

[10] G. Martinelli, S. Simula and L. Vittorio, *$|V_{cb}|$ and $R(D^{(*)})$ using lattice QCD and unitarity*, *Phys. Rev. D* **105** (2022) 034503 [2105.08674].

[11] G. Martinelli, S. Simula and L. Vittorio, *Exclusive semileptonic $B \to \pi \ell \nu_\ell$ and $B_s \to K \ell \nu_\ell$ decays through unitarity and lattice QCD*, *JHEP* **08** (2022) 022 [2202.10285].

[12] JLQCD collaboration, *Form factors of $B \to \pi \ell \nu$ and a determination of $|V_{ub}|$ with Möbius domain-wall fermions*, *Phys. Rev. D* **106** (2022) 054502 [2203.04938].

[13] BaBar collaboration, *Study of $B \to \pi \ell \nu$ and $B \to \rho \ell \nu$ decays and determination of $|V_{ub}|$*, *Phys. Rev. D* **83** (2011) 032007 [1005.3288].

[14] BaBar collaboration, *Branching fraction and form-factor shape measurements of exclusive charmless semileptonic B decays, and determination of $|V_{ub}|$*, *Phys. Rev. D* **86** (2012) 092004 [1208.1253].

[15] Belle collaboration, *Measurement of the decay $B^0 \to \pi^- \ell^+ \nu$ and determination of $|V_{ub}|$*, *Phys. Rev. D* **83** (2011) 071101 [1012.0090].

[16] Belle collaboration, *Study of exclusive $B \to X_u \ell \nu$ decays and extraction of $|V_{ub}|$ using full reconstruction tagging at the Belle experiment*, *Phys. Rev. D* **88** (2013) 032005 [1306.2781].